


Exosomal miR-450b-5p Secreted from Exendin-4-Stimulated Endothelial Cells Protects Retinal Ganglion Cells Against Ischemia Reperfusion Injury

Yanan Sun^{1,2,*}, Ruyi Zhai^{1,*}, Qilian Sheng^{1,*}, Yue Ying^{1,*}, Ye Lin Kwan¹, Xintong Fan¹, Huan Xu¹, Xiangmei Kong¹

¹Eye Institute and Department of Ophthalmology, Eye & ENT Hospital, Fudan University, National Health Commission Key Laboratory of Myopia (Fudan University), Key Laboratory of Myopia, Chinese Academy of Medical Sciences, Shanghai Key Laboratory of Visual Impairment and Restoration, Shanghai, People's Republic of China; ²Shenzhen Eye Hospital, Shenzhen Eye Medical Center, Southern Medical University, Shenzhen, People's Republic of China

*These authors contributed equally to this work

Correspondence: Xiangmei Kong; Huan Xu, Eye Institute and Department of Ophthalmology, Eye & ENT Hospital, Fudan University, 83 Fenyang Road, Xuhui District, Shanghai, 200031, People's Republic of China, Tel +86 2164377134, Email kongxm95@163.com; xuhuan320@163.com

Background: Retinal ischemia-reperfusion (RIR) injury represents a critical pathophysiological mechanism underlying various ocular ischemic diseases, characterized by progressive loss of retinal ganglion cells (RGCs). Exendin-4 (Ex-4), a widely used glucagon-like peptide-1 receptor (GLP-1R) agonist drug in the treatment of type 2 diabetes mellitus, has been reported to protect against ischemia-reperfusion (IR) injury in various vital organs. However, the potential neuroprotective effect of Ex-4 under RIR injury has been poorly understood.

Methods: Immunofluorescence staining assay, hematoxylin and eosin (HE) staining were conducted to evaluate the neuroprotective role of Ex-4. A co-culture assay of human retinal vascular endothelial cells (HRVECs) and RGCs was established. Extracellular vesicles (EVs) were isolated from the culture supernatant of HRVECs with (E-EVs) or without Ex-4 treatment (O-EVs) under oxygen-glucose deprivation/reoxygenation (OGD/R) condition. Transmission electron microscopy (TEM), Nanoparticle tracking analysis (NTA) and Nano-flow cytometry (NanoFCM) were used to detect the presence and purity of EVs. Cell activity, reactive oxygen species (ROS) level, and cell death rate of RGCs were evaluated. Further global miRNA sequencing was performed on E-EVs or O-EVs to explore potential mechanisms.

Results: Our findings revealed that Ex-4 had a GLP-1R-dependent neuroprotective effect on RGCs. Vascular endothelial cells (VECs) -derived EVs mediate the protective effect of Ex-4 on RGCs under acute RIR injury. We identified miR-450b-5p as a highly enriched miRNA in E-EVs. Treatment with either E-EVs or miR-450b-5p mimics significantly protected RGCs against RIR-induced injury. Mechanistic investigations identified acyl-coenzyme A (CoA) synthetase long-chain family member 4 (ACSL4) as a direct target of miR-450b-5p.

Conclusion: Ex-4 exerts its neuroprotective effects under RIR injury by stimulating retinal VECs to secrete miR-450b-5p-enriched EVs, thereby revealing a novel endothelial-mediated neuroprotective pathway in ischemia diseases.

Keywords: exendin-4, retinal ganglion cells, ischemia reperfusion injury, retinal vascular endothelial cells, extracellular vesicles, microRNA

Introduction

Ischemia-reperfusion (IR) injury is characterized by an initial limitation of blood supply followed by the subsequent restoration of perfusion.¹ IR injury is a common pathological process responsible for a wide range of clinical conditions,

including stroke, organ transplantation, heart attack, and several retinal ischemic diseases such as glaucoma, central retinal artery occlusion, and diabetic retinopathy.^{2,3} Retinal ischemia-reperfusion (RIR) injury is histologically manifested by loss of retinal ganglion cells (RGCs), which eventually leads to visual impairment or blindness.⁴ Rapid occlusion of retinal blood flow initiates a detrimental cascade involving calcium influx and compromise of the blood-retina barrier (BRB) integrity.⁵ Further, the restoration of blood flow induces a substantial surge of reactive oxygen species (ROS) and triggers inflammatory cascades, ultimately resulting in loss of RGCs.^{6,7} However, the molecular pathogenesis of RGC damage under RIR injury has not been fully elucidated.

Glucagon-like peptide-1 (GLP-1) and its analogs are first-line hypoglycemic agents that are widely used in clinic.⁸ The GLP-1 receptor (GLP-1R) agonist exendin-4 (Ex-4) is a long-acting analog of GLP-1. Beyond glucose-lowering, emerging evidence highlights the protective effects of Ex-4 against IR injury in vital organs such as heart, kidney, and brain.^{9–12} In our previous study, we demonstrated the expression of GLP-1R in human retinal vascular endothelial cells (HRVECs). Ex-4 could significantly alleviate the retinal microvascular occlusion induced by RIR injury, demonstrating the retinal vasoprotective effect of Ex-4.¹³ Ferreira et al demonstrated that Ex-4 could cross the blood-brain barrier (BBB), ameliorate brain tissue infarction, and attenuate neuronal cell death in an ischemic-hypoxic encephalopathy model.¹⁴ The neuroprotective effects of GLP-1R agonists in Alzheimer's disease and Parkinson's disease have also been demonstrated.^{15,16} However, evidence is lacking regarding whether Ex-4 has neuroprotective effects in acute RIR or glaucoma models.

Vascular endothelial cells (VECs) are important components of the BRB and locate near the neurons.¹⁷ VECs play a crucial role in maintaining neuronal homeostasis through bidirectional nutrient exchange, metabolic waste removal, and secretion of bioactive molecules via angiocrine.¹⁸ However, most VECs-derived bioactive molecules do not directly modulate neuronal function. Accumulating evidence suggests that extracellular vesicles (EVs), particularly the exosome subclass, secreted by VECs play a pivotal role in intercellular communication.¹⁹ These EVs function as carriers of bioactive components, such as microRNAs (miRNAs) and proteins, delivering them to recipient cells.²⁰ Owing to their lipid membrane structure, EVs have potential neuroprotective effects via transcytosis across barrier structures.²¹ Venkat et al revealed that neurons internalize exosomes secreted by brain VECs in a mouse stroke model.²² Yue et al found that VECs derived exosomes exert neuroprotective effects on hippocampal neurons against oxygen-glucose deprivation (OGD)-induced injury.²³ Collectively, these findings indicate that EVs may be one of the important mechanisms mediating VEC-neuron interactions.

Our previous study demonstrated a retinal vasoprotective effect of Ex-4 under RIR injury. However, whether Ex-4 has neuroprotective effects in acute RIR or glaucoma models has not yet been elucidated. In this study, we hypothesize that EVs from VECs mediated the neuroprotective effect of Ex-4 under RIR injury by transferring specific miRNAs. We further explored the potential neuroprotective mechanisms of Ex-4, aiming to broaden its clinical utility in the treatment of nerve injury in IR-related conditions.

Materials and Methods

Sex as a Biological Variable

6–8 weeks male C57BL/6J mice were used in this study. Male mice were selected to eliminate potential confounding effects from hormonal variations in females.

Animals

C57BL/6J male mice (6–8 weeks old) were purchased from Hangzhou Ziyuan Animal Center. All procedures were conducted in compliance with the ARVO Statement on the Use of Animals in Ophthalmic and Vision Research. All animals were housed in a temperature-controlled environment ($22 \pm 1^\circ\text{C}$) with a 12-hour light/dark cycle and provided with free access to food and water. The mice were group-housed (3–5 animals per cage) in polycarbonate cages containing sterilized aspen wood chip bedding. Mice were randomly selected for treatment and observed without prior knowledge of the treatment.

Experimental Animals

The mice were anesthetized with 1% sodium pentobarbital intraperitoneal (50 mg/kg) injection. Tropicamide eye drops and oxybuprocaine hydrochloride eye drops (Santen, Japan) were applied locally to the eye for pupil dilation and topical anaesthetization, respectively. A 33-gauge needle was cannulated into the anterior chamber to sustain intraocular pressure (IOP) at 70–80 mmHg for 60 min. Tonometer (TonoLab, ICare) was used to measure the IOP. Tobramycin ointment was used to prevent bacterial infection. The mice were housed in a warm and clean environment for 24 h to allow for fundus blood flow reperfusion. Eight mice were initially assigned to each experimental group. Animals exhibiting ductal slippage or other surgical complications during high-pressure ischemia induction were excluded to ensure model validity. Final group sizes ranged from 4–5 animals that successfully completed the protocol. Following successful acute RIR model establishment, animals were randomly divided into six experimental subgroups with balanced numbers: Control (Ctr), RIR model (RIR+PBS), RIR+Ex-4 (1 $\mu\text{g}/\mu\text{L}$), RIR+Ex-4 (1 $\mu\text{g}/\mu\text{L}$) + Ex-9-39 (4 $\mu\text{g}/\mu\text{L}$), RIR + O-EVs (1×10^7 particles/ μL), RIR + E-EVs (1×10^7 particles/ μL). Retinas were harvested 7 days post-RIR treatment, and the samples were fixed and stored at specific temperatures for subsequent imaging or biochemical analyses.

Cell Isolation and Culture

Immunopanning with CD90 antibody (Bio-Rad, USA) was used to purify primary RGCs from 1-day postnatal C57BL/6J mice. Retinas were dissociated with papain (Worthington, USA). Anti-macrophage antibody (Cedarlane, USA) was used to remove the contaminating macrophages and endothelial cells. Then, anti-CD90 antibody was used to immunologically selected RGCs from macrophage-depleted cell suspensions. Finally, the RGCs were collected and plated on matrigel-coated 48 or 96-well tissue culture plates at 37°C for 24 h in 10% CO₂ until they were completely adherent. Preparation of RGC culture medium: Neurobasal (Life Technologies) supplemented with brain-derived neurotrophic factor (BDNF; 50 ng/mL), ciliary neurotrophic factor (CNTF; 10 ng/mL), forskolin (5 mM), triiodothyronine (T3; 40 ng/mL), sodium pyruvate (1 mM), L-glutamine (1 mM), insulin (5 mg/mL), N-acetyl cysteine (5 mg/mL), and N27 (1:100) as described.^{24,25} HRVECs (cAP-0010, Angio-Proteomien) were cultured in endothelial growth medium (ECM, 1001; ScienCell) supplemented with 10% FBS and 1% PS (penicillin/streptomycin) in 5% CO₂ at 37°C.

Establishment of the OGD/R Model

The oxygen-glucose deprivation/reoxygenation (OGD/R) model was adopted in this study as it represents a well-established in vitro system for investigating RIR injury.²⁶ To construct the OGD/R model, cells were washed twice with PBS and then cultured with glucose-free Dulbecco's modified Eagle medium (DMEM) (Gibco). Next, the cells were placed in a modular incubator chamber set under hypoxic conditions (1% O₂, 94% N₂, and 5% CO₂) at 37°C for 4 h. Then, the DMEM was removed and the ECM medium administered with (or without) the addition of Ex-4 (10 nM) was added to incubate HRVECs under conditions of normoxia (21% O₂, 5% CO₂) for a period of 24 h.

Isolation and Characterization of EVs

After OGD/R treatment, HRVECs was cultured with exosome-depleted FBS for another 48 h. The medium was collected and centrifuged at 2000 g at 4°C for 10 min to remove the cell debris. Next, the supernatants were filtered through 0.45 μm and 0.22 μm filter. Exo Quick-TC EV Precipitation Solution (System Biosciences, Palo Alto) was used to isolate EVs from the cell culture medium.²⁷ The final exosome pellets were resuspended in 60–80 μL PBS and stored at -80°C for further experiments needs. EVs isolated by precipitation were comparable in size, markers, miRNA content, and functional activity to those obtained by ultracentrifugation.²⁸ Transmission electron microscopy (TEM) and Nanoparticle tracking analysis (NTA) were used to examine the morphology and size distribution of the EVs. The markers of EVs including anti-CD9 (sc-7637; 1:100) and anti-CD81 (1:100, sc-5275) were assessed by Nano-flow cytometry (NanoFCM).

Fluorescent Labeling of EVs

According to the manufacturer's instructions, EVs were incubated with PKH67 membrane dye (4 μ L, Sigma-Aldrich) and Diluent C for 4 min. Labeled EVs were precipitated with Exo Quick-TC (System Biosciences, Palo Alto), incubated overnight at 4°C, and centrifuged 10 min at 10,000 rpm to clear out the unbound PKH67 dye, followed by suspension in PBS.

EVs Uptake Analysis

RGCs were treated with labeled-EVs for 4 h, followed by fixation with 4% paraformaldehyde for 30 min. Nuclei were counterstained with 4',6-diamidino-2-phenylindole (DAPI; Sigma-Aldrich). Images were obtained using a fluorescence microscope (Zeiss, LSM700B).

miRNA Array

According to the manufacturer's protocol, total RNA was extracted using exoRNeasy Kit (QIAGEN, USA) and then quantified by using NanoDrop (ND-2000, Thermo Scientific). The RNA integrity was assessed by RNA 6000 Nano Lab Chip Kit (Agilent, USA). TruSeq Small RNA Sample Prep Kit (Illumina, San Diego, USA) was used to prepare the small RNA library. Single-end sequencing on an Illumina HiSeq2500 at LC-BIO (Hangzhou, China) was performed following the vendor's recommended protocol. An Agilent Microarray Scanner was used to scan the slides using the default settings. Raw reads were analyzed using the ACGT101-miR program (LC Sciences, USA).

CCK-8 Assay

CCK-8 solution (10 μ L; Dojindo Laboratories) was added to each well of 96-well plate and incubated with the cells for 4 h at 37°C. The absorbance was measured at 450 nm wavelength using a microplate reader (Tecan; Infinite M1000).

ROS Detection

After incubation with 2',7'-Dichlorodihydrofluorescein diacetate (DCFH-DA, Beyotime, China) for 20 min at 37°C, RGCs were gently washed three times with PBS. Images were acquired using a Zeiss microscope (Zeiss, Germany), and fluorescence intensities were analyzed using ImageJ.

Propidium Iodide (PI)/Calcein-AM Staining

RGCs were gently washed three times with PBS and then incubated with Calcein-AM (10 μ M, C3099) and PI (10 μ M, P3566) at 37°C for 20 min. Images of live and dead cells were acquired using a fluorescence microscope (Zeiss, Germany) with an excitation filter of 490 nm or 545 nm.

RT-qPCR

RNA was extracted from EVs by using Total RNA Kit (TianGen). For miRNAs, cDNA was synthesized using poly-A tail extension by miRcute Plus miRNA First-Strand cDNA Kit (TianGen). miRcute Plus miRNA qPCR Kit with SYBR Green (TianGen) was used to quantify the expression of miRNA. The miRNA-450b-5p primers used were as follows: forward, TGGTACTCGGAGAGAGGTTACCC.

Optical Coherence Tomography (OCT)

The thickness of the ganglion cell layer (GCL) and inner plexiform layer (IPL) were measured using OCT (Optoprobe Science, ISOCT, UK).

Quantification of RGC Survival in vivo

On day 7 after reperfusion, eyeballs were fixed in 4% PFA for 30 min at room temperature. Whole-mount retinal eyecups were permeabilized and blocked with 5% BSA and 1% Triton for 30 min. Primary antibodies against the Brn3a/Pou4f1 transcription factor (Brn3a, 1:300, #SC-8429, Santa Cruz Biotechnology) or the RNA-binding protein with multiple splicing (RBPMS, 1:200, Cat#ab152101, Abcam) were used to label RGCs and assess loss of RGCs. The retinal whole-

mount was incubated with anti-rabbit Alexa Fluor 488 (1:1000, ab150077, Abcam) for 2 h at room temperature. The image was examined using a Zeiss microscope (Zeiss, Germany).

Histological Examination

On day 7 after reperfusion, eyes were collected, fixed in formalin, and embedded in paraffin and sections (5 μm) of each eye were prepared. Morphometric analysis was performed to quantify RIR injury by hematoxylin and eosin (H&E) staining. The ganglion cell layer and inner plexiform layer (GCL+IPL) thickness were measured using the ImageJ software.

Statistics

Data are reported as mean \pm standard deviation (SD). The data were processed and analyzed using SPSS software (version 16.0). One-way ANOVA and Student's t test were employed where suitable, with a significance level set at $*P < 0.05$.

Study Approval

The experimental procedures and all animal care were approved by the EENT Hospital of Fudan University and in accordance with the guidelines for the Care and Use of Laboratory Animals published by the United States National Institutes of Health.

Data Availability

The datasets used and/or analyzed during the current study are available from the corresponding author upon reasonable request.

Results

Ex-4 Protects Against RIR-Induced RGC Damage via GLP-1R-Dependent Pathway

The loss of RGCs is considered as a hallmark of neurodegeneration following RIR injury. To initially evaluate the neuroprotective potential of Ex-4, we administered Ex-4 (1 $\mu\text{g}/\mu\text{l}$) via intravitreal injection 24 hours following RIR induction. Seven days post-induction, retinal histological changes were evaluated using H&E staining. RIR injury induced significant thinning of inner retinal layers, particularly the GCL+IPL thickness. Ex-4 treatment attenuated RIR-induced inner retinal structural damage compared to the RIR group (Figure 1A). Consistent findings were obtained through OCT analysis, which corroborated the neuroprotective effects observed histologically (Figure 1B). The Brn3a is selectively expressed by cells in the GCL, serves as a reliable marker for detecting significant changes in RGC survival.²⁹ Brn3a immunostaining of retinal wholemounts revealed that Ex-4 treatment significantly attenuated RIR-induced RGC death (Figure 1C). Collectively, these results demonstrate that Ex-4 treatment effectively attenuates RIR-induced inner retina structural damage and prevents loss of RGCs, confirming its neuroprotective effect against RIR injury.

To further evaluate whether Ex-4 exhibit its neuroprotective role through binding to the GLP-1R, Exendin-9-39 (Ex-9-39, 4 $\mu\text{g}/\mu\text{l}$), a GLP-1R antagonist, was co-injected intravitreally with Ex-4. Our results demonstrate that pharmacological blockade of GLP-1R by Ex-9-39 reversed Ex-4's neuroprotective effects on RIR-induced damage, confirming the critical requirement of GLP-1R activation (Figure 1A–C).

Ex-4 Has No Direct Protective Effect on RGCs Under OGD/R Injury

Immunofluorescence assay was used to assess whether GLP-1R was present in mouse RGCs. RBPMS serves as a well-established marker for sensitive and specific detection of RGC. We found that GLP-1R was not co-expressed with RBPMS of RGCs in vivo (Figure 2A). The OGD/R model was adopted as it represents a well-established in vitro system for investigating RIR injury. We further investigated whether Ex-4 exerts direct protective effects on RGCs under OGD/R injury. Following a 4 h period of ischemia and a 24 h period of reperfusion, the relative viability of RGCs decreased to approximately 50% (Figure 2B), the ROS level increased by 1.4-fold (Figure 2C), and the death rate of RGCs increased by 3.4-fold (Figure 2D) compared to the Ctr group. No significant improvements were observed following Ex-4 (10 nM)

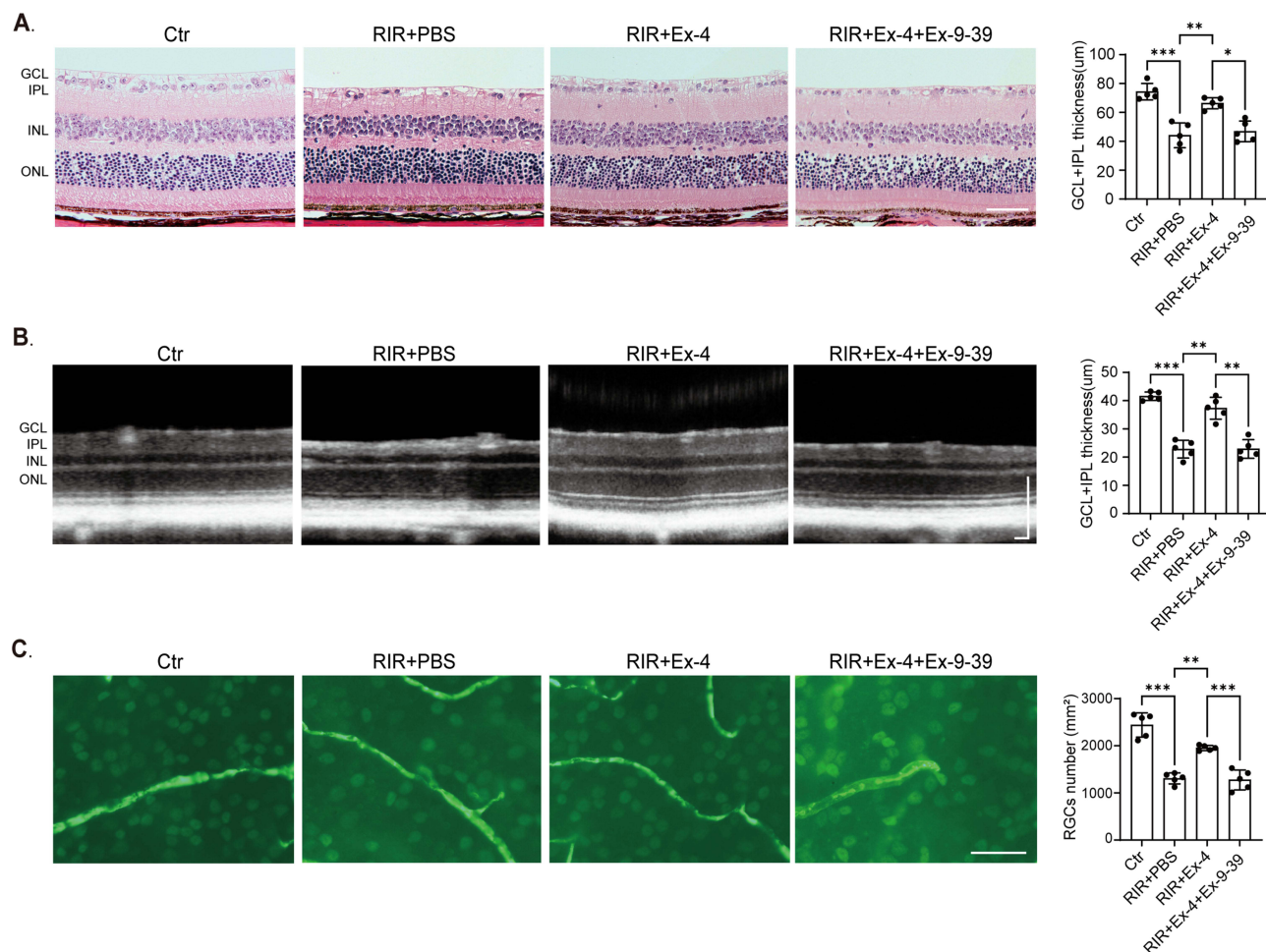


Figure 1 Ex-4 protects against RIR-induced RGC damage via GLP-1R-dependent pathway. The mice were treated with Ex-4 one day after IR insult. **(A)** Representative hematoxylin and eosin (H&E) images of retinal section. $n=5$ for each group. Thickness of GCL+IPL was measured. Scale bars: $50\ \mu\text{m}$. **(B)** Representative OCT scans in living mice. Thickness of GCL+IPL was measured. $n=5$ for each group. Scale bars: $100\ \mu\text{m}$. **(C)** Representative retinal mounts with fluorescent staining of RGCs. The number of RGCs was measured. $n=5$ for each group. Scale bars: $50\ \mu\text{m}$. * $P < 0.05$; ** $P < 0.01$, *** $P < 0.001$. Data were presented as mean \pm SD. Statistical significance was determined by one-way ANOVA.

treatment regarding reduced cellular activity, increased ROS level or cell death rate, indicating that Ex-4 have no direct protective effect on RGCs under OGD/R injury.

VECs-EVs Mediate the Protective Effect of Ex-4 on RGCs Under OGD/R Injury

We hypothesize that VECs may mediate the protective effects of Ex-4 on RGCs. We established a co-culture system for HRVECs and RGCs and found that HRVECs treated with Ex-4 (24 h) and co-cultured with RGCs could significantly ameliorate RGCs injury induced by OGD/R, as evidenced by increased cell viability (Figure 3A), decreased ROS levels (Figure 3B), and lower neuronal dead rate (Figure 3C and D).

Accumulating evidence suggests that extracellular vesicles (EVs) secreted by VECs play a pivotal role in intercellular communication. GW4869, a neutral sphingomyelinase inhibitor, was employed as an inhibitor to specifically block the secretion of EVs.³⁰ To investigate whether EVs mediate the neuroprotective effects of Ex-4-treated VECs (Ex-4/VECs) on RGCs, we established a co-culture system of Ex-4/VECs with or without GW4869 and RGCs under OGD/R injury. The results indicated that the neuroprotective effect of Ex-4/VECs was partially abolished by the addition of GW4869 (Figure 3A–D).

To further investigate the direct neuroprotective effects of Ex-4/VECs, we subsequently isolated EVs from the culture supernatant of HRVECs under OGD/R injury, with Ex-4 (E-EVs) or without Ex-4 treatment (O-EVs). NTA showed that the

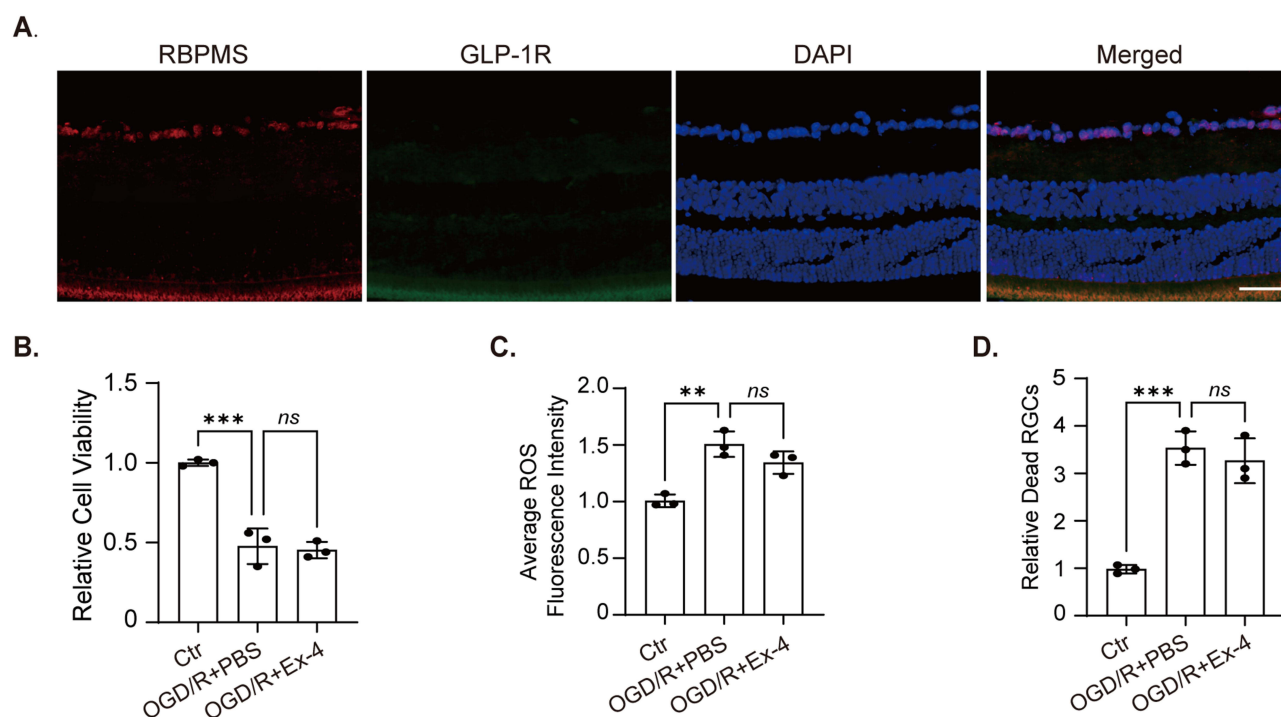


Figure 2 Ex-4 has no direct protective effect on RGCs under OGD/R injury. **(A)** Retinal ganglion cells labeled with RBPMS antibodies (red), GLP-1R antibodies (green) and DAPI staining indicates the cell nucleus (blue) in retinal slide. Scale bar: 50 μ m. **(B)** CCK-8 assays were conducted to detect the viability of RGCs. $n=3$ for each group. **(C)** The ROS level was measured through the fluorescent probe, DCFH-DA, and the ratio of ROS⁺ cells were measured. $n=3$ for each group. **(D)** Cell death rate was determined using PI/Calcein-AM double staining. $n=3$ for each group. ** $p < 0.01$; *** $p < 0.001$. Data were presented as mean \pm SD. Statistical significance was determined by one-way ANOVA.

diameter distribution of EVs was within the range of 30–120 nm (Figure 3E). NanoFCM detected the positive markers CD9 and CD81 on the surface of EVs (Figure 3F). TEM showed that the isolated EVs had a typical saucer-like shape and double-layer membrane structure (Figure 3G). Then we labeled VECs-derived EVs with PKH67, and incubated primary RGCs with PKH67-labeled EVs. We found that RGCs efficiently consumed PKH67-labeled EVs, mainly in the cell bodies (Figure 3H).

EVs Secreted from Ex-4/VECs Protect RGCs from RIR Injury

To evaluate the neuroprotective role of E-EVs under RIR injury in vivo, EVs (1×10^7 particles/ μ L) were administered intravitreally 24 h after reperfusion. As shown in Figure 4A, E-EVs administration partially restored the inner retinal structure damage compared to that in the RIR+O-EVs group. Immunostaining of retinal wholemounts for RBPMS showed that E-EV treatment rescued RGC death with a 20% increase compared with the RIR+O-EVs group (Figure 4B). We further extend our observation to primary RGCs under OGD/R condition. We incubated RGCs with E-EVs or O-EVs for 24 h after OGD treatment in vitro. PI/Calcein-AM staining assay showed that incubation with E-EVs decreased the death rate of RGCs (Figure 4C). Moreover, we found increased viability (Figure 4D) and decreased level of ROS (Figure 4E) in OGD/R-treated RGCs incubated with E-EVs.

VECs-EVs Content miR-450b-5p Mediating the Protective Effect of Ex-4 on RGCs Under OGD/R Injury

We employed Agilent miRNA microarray analysis to systematically identify candidate miRNAs potentially responsible for E-EVs-induced neuroprotection effects against OGD/R injury. A total of 1647 miRNAs were identified and 15 miRNAs were differentially expressed between O-EVs and E-EVs (Figure 5A). RT-PCR showed that miR-450b-5p was highly enriched in the E-EVs compared to O-EVs (Figure 5B). To validate whether miR-450b-5p mediates the neuroprotective effects of E-EVs, we transfected primary RGCs with miR-450b-5p mimics. After incubation with Cy3-miR-450b-5p for 6 h, more than 80% of RGCs exhibiting positive Cy3 fluorescence (Figure 5C). Overexpression of miR-450b-5p showed a protective effect on RGCs under

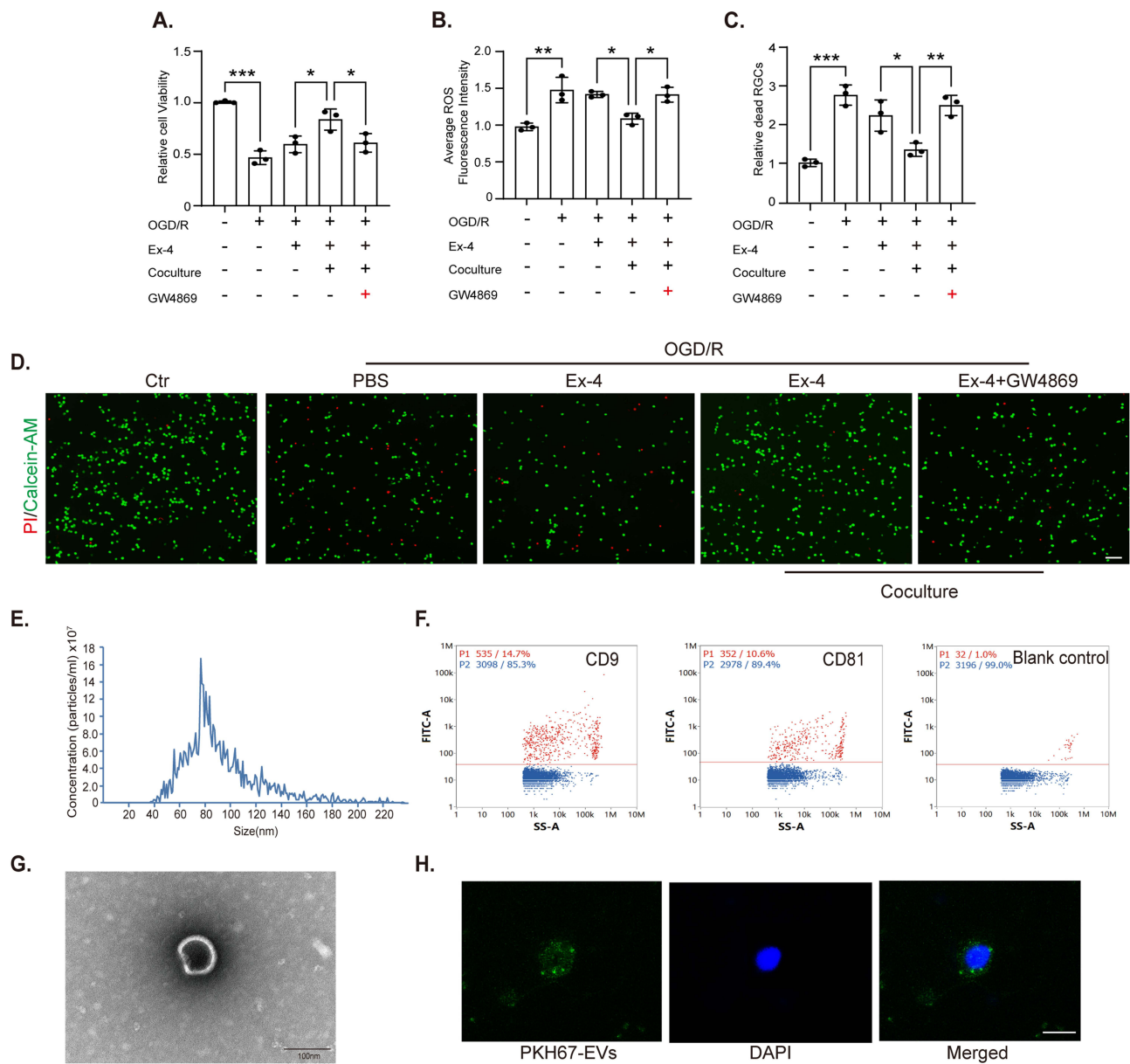


Figure 3 VECs-EVs mediate the protective effect of Ex-4 on RGCs under OGD/R injury. **(A)** CCK-8 assays were conducted to detect the viability of RGCs. $n=3$ for each group. **(B)** The ROS level was measured through the fluorescent probe, DCFH-DA, and the ratio of ROS⁺ cells were measured. **(C and D)** RGC death rate was determined by PI/Calcein-AM double staining. $n=3$ for each group. Scale bar: 50 μ m. **(E)** The size of EVs was assessed by NTA. **(F)** Positive markers CD9 and CD81 on the surface of exosomes was detected by NanoFCM. **(G)** Characterization of EVs isolated from VECs by TEM. **(H)** Ex-4/VECs derived EVs were labeled with PKH67 and incubated with primary RGCs for 4 h. Scale bar: 5 μ m. * $P < 0.05$; ** $P < 0.01$; *** $P < 0.001$. Data were presented as mean \pm SD. Statistical significance was determined by one-way ANOVA.

OGD/R injury like that of E-EVs. The result showed that miR-450b-5p mimic treatment increased the cell viability (Figure 5D), decreased ROS level (Figure 5E) and the death rate (Figure 5F) of RGCs under OGD/R injury compared with that in NC-treated group. These findings indicated that miR-450b-5p could act as a mediator of the E-EV-induced protective role of RGCs under OGD/R injury.

Exosomal miR-450b-5p Reduces Neuronal Damage Under OGD/R Injury by Targeting ACSL4

Compelling evidence from recent studies has established ACSL4 as a key mediator of IR injury in various organs, particularly in the brain, heart and intestine.^{31–33} Nevertheless, the involvement of ACSL4 in RIR injury has not yet been experimentally

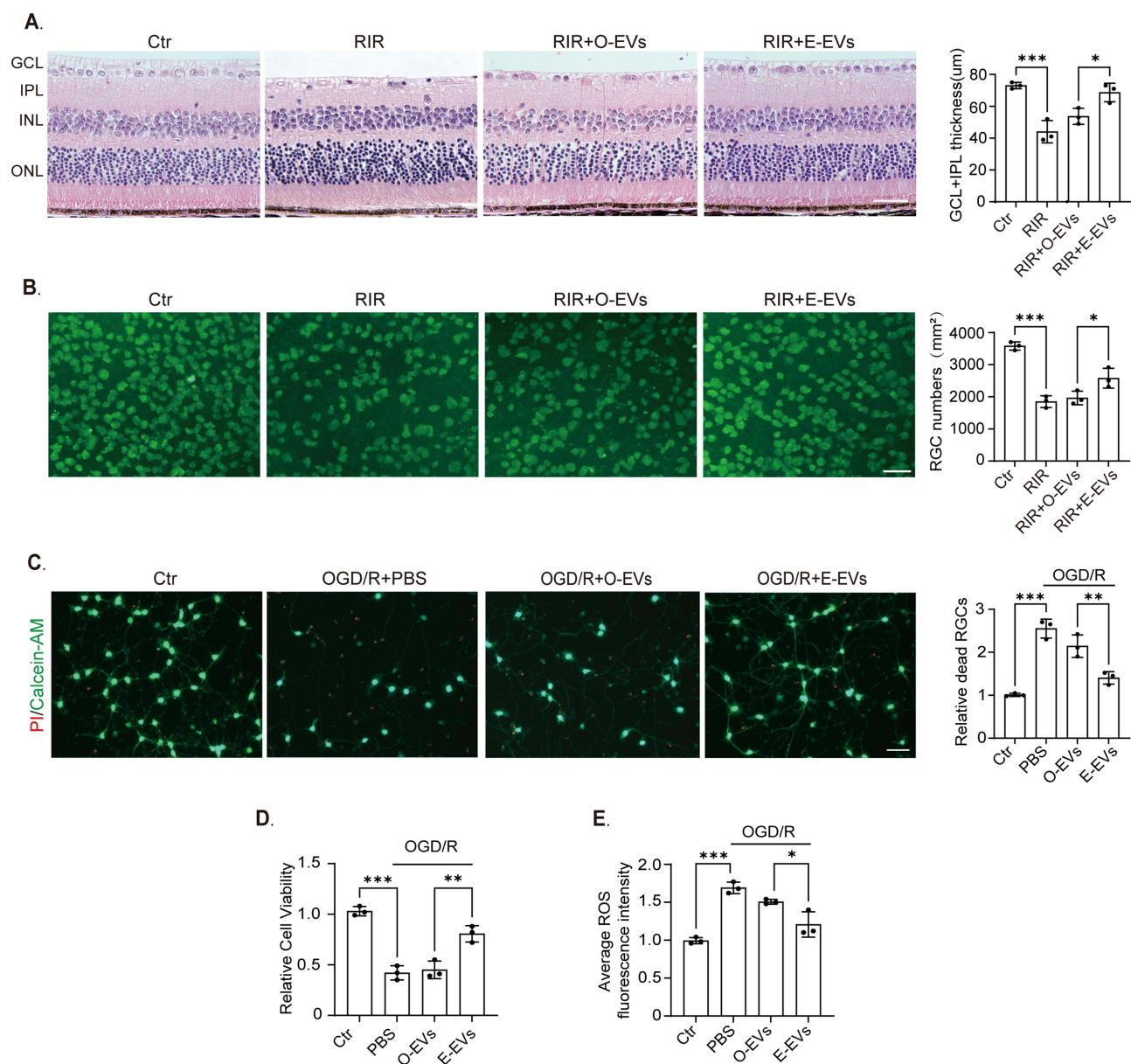


Figure 4 EVs secreted from Ex-4/VECs protect RGCs from RIR injury. **(A)** Representative H&E images of retinal section. n=3 for each group. Scale bars: 50 μm. **(B)** Representative retinal mounts with RBPMs fluorescent staining of RGCs. n=3 for each group. Scale bars: 50 μm. **(C)** RGC death rate was determined by PI/Calcein-AM double staining. n=3 for each group. Scale bar: 50 μm. **(D)** CCK-8 assays were conducted to detect the viability of RGCs. n=3 for each group. **(E)** The ROS level was measured through the fluorescent probe, DCFH-DA, and the ratio of ROS⁺ cells were measured. n=3 for each group. *P < 0.05; **P < 0.01; ***P < 0.001. Data were presented as mean ± SD. Statistical significance was determined by one-way ANOVA.

validated. Using the RNAhybrid software, we observed a low binding free energy between miR-450b-5p and ACSL4, indicating a stable binding tendency.³² To investigate the interaction between miR-450b-5p and ACSL4 under OGD/R conditions in RGCs, we transfected miR-450b-5p mimic and detected ACSL4 expression. As shown in Figure 6A, miR-450b-5p overexpression suppressed the expression of ACSL4. We further clarified mechanistic insights into the regulatory effect of E-EVs content miR-450b-5p. Compared to the Ctr group, OGD/R injury increased Fe²⁺ and ROS level, whereas miR-450b-5p mimic or si-ACSL4 remarkably resisted neuronal damage in RGCs under OGD/R injury, as indicated by decreased Fe²⁺ (Figure 6B) and ROS levels (Figure 6C). Collectively, these results suggest that EVs secreted from Ex-4-stimulated VECs protects RGCs against RIR injury through miR-450b-5p/ACSL4 pathway.

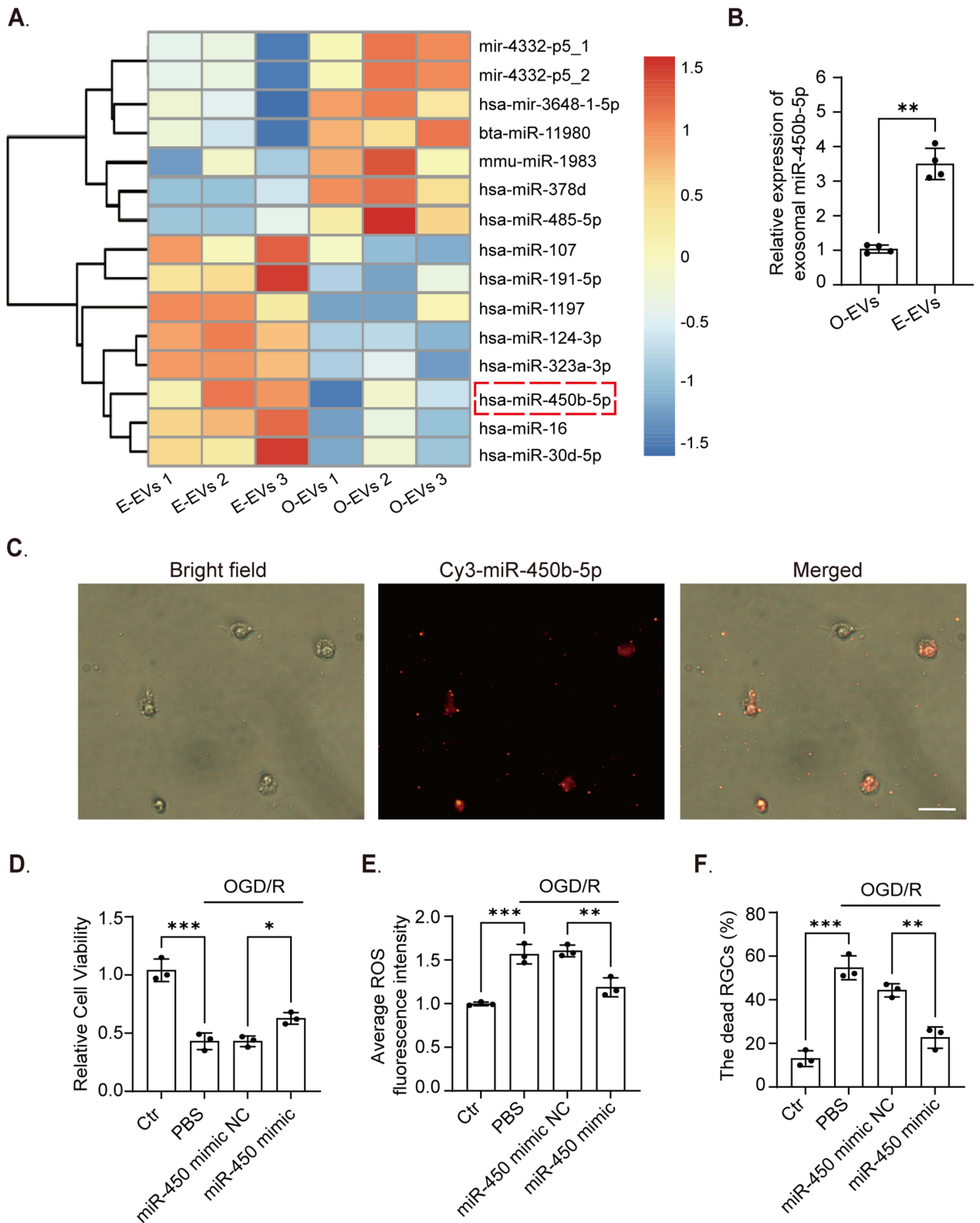


Figure 5 VECs-EVs content miR-450b-5p mediate the protective effect of Ex-4 on RGCs under OGD/R injury. **(A)** A heatmap showing the differentially expressed miRNAs (fold change ≥ 1.5 ; $*P < 0.05$) between O-EVs and E-EVs. $n=3$ biologically independent samples per group. **(B)** qRT-PCR analysis of miR-450b-5p expression in O-EVs and E-EVs. $n=4$ for each group. **(C)** Cy3-miR-450b-5p were incubated with RGCs for 6 h and observed under a fluorescence microscope. Scale bar: 20 μm . **(D)** CCK-8 assays were conducted to detect the viability of RGCs with miR-450b-5p mimic treatment. $n=3$ for each group. **(E)** The ROS level was measured through the fluorescent probe, DCFH-DA, and the ratio of ROS⁺ cells were measured. $n=3$ for each group. **(F)** RGC death rate was determined by PI/Calcein-AM double staining with miR-450 mimic treatment. $n=3$ for each group. $*P < 0.05$; $**P < 0.01$; $***P < 0.001$. Data were presented as mean \pm SD. Statistical significance was determined by one-way ANOVA.

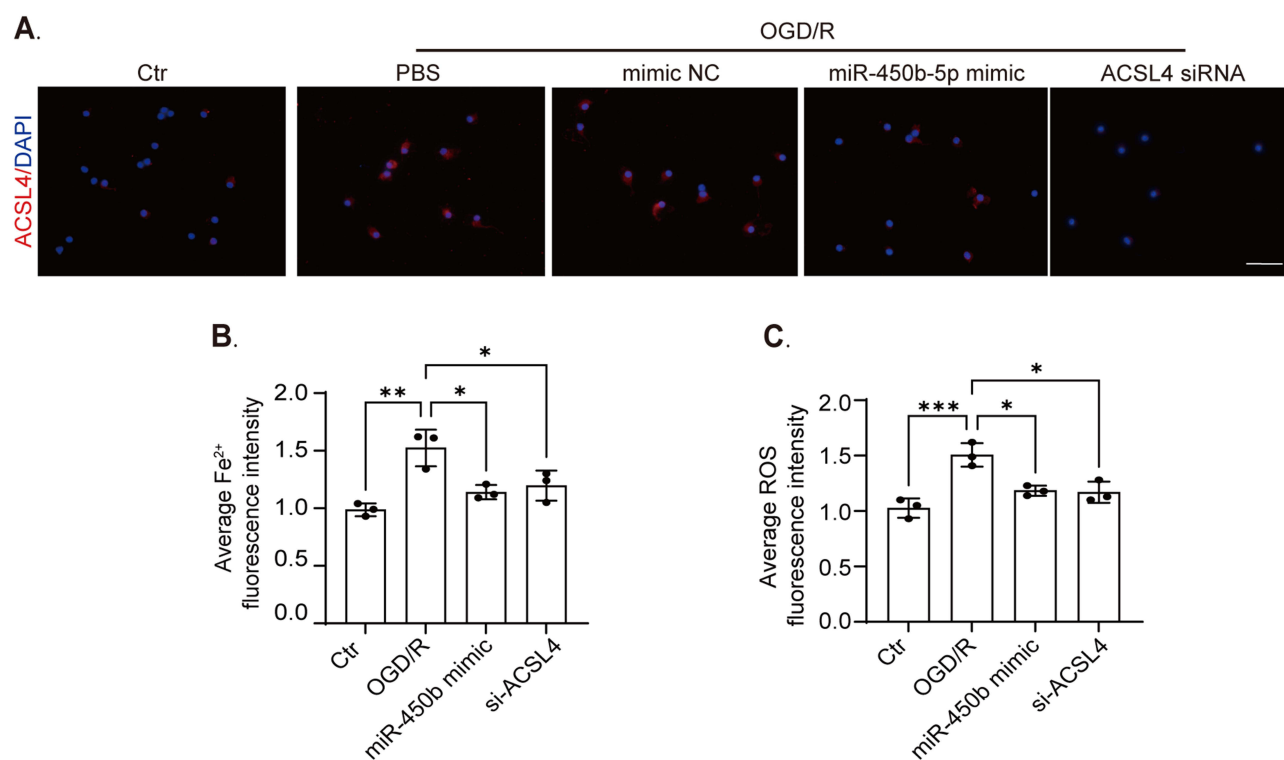


Figure 6 Exosomal miR-450b-5p reduces neuronal damage under OGD/R injury by targeting ACSL4. **(A)** Immunofluorescence images of RGCs stained with ACSL4 (Red) and DAPI (Blue). Scale bar, 10 μm. **(B)** miR-450b-5p mimic or si-ACSL4 reduced Fe²⁺ levels in RGCs under OGD/R injury. n=3 for each group. **(C)** The ROS level was measured through the fluorescent probe, DCFH-DA, and the ratio of ROS⁺ cells were measured. n=3 for each group. *P < 0.05; **P < 0.01; ***P < 0.001. Data were presented as mean ± SD. Statistical significance was determined by one-way ANOVA.

Discussion

IR injury represents a critical pathophysiological mechanism in a wide range of pathologies, including myocardial infarction, ischemic stroke, acute kidney injury, trauma, and various retinal ischemic disorders.³⁴ Thus, it is essential to identify new functional targets or drugs for rescuing IR injury. Our previous study demonstrated a retinal vasoprotective effect of Ex-4 under RIR injury.¹³ However, whether Ex-4 has neuroprotective effects in acute RIR or glaucoma models has not yet been elucidated. In this study, we noted the neuroprotective effect of Ex-4 under RIR injury. The present study delineated a novel paracrine protective mechanism whereby Ex-4 protected RGCs under OGD/R condition through its modulation of VEC function, suggesting a neurovascular unit-mediated pathway of protection.

Retinal tissue is extremely metabolic, and the blood supply to visual neurons comes mainly from the retinal blood vessels in the terminal branches, which are severely affected by ischemia. Once retinal ischemia occurs, it induces progressive loss of RGCs and results in significant visual dysfunction. Current researches illustrated that Ex-4 has neuroprotective effect against IR injury in various vital organs. Teramoto et al found that Ex-4 exerts neuroprotective effects in the brain following IR injury by inhibiting oxidative DNA damage, lipid peroxidation and the activation of microglia.³⁵ Shan et al demonstrated that Ex-4 ameliorates the inflammatory response induced by cerebral ischemia and disruption of the BBB in an astrocyte-dependent manner.³⁶ Xie et al found that Ex-4 could reduce neuronal apoptosis through the GLP-1R/PI3K/Akt signaling pathway and ameliorate IR-induced brain neurological damage.³⁷ However, the neuroprotective effects of Ex-4 in acute RIR-induced RGCs damage and its underlying mechanisms remain incompletely understood. In the present study, we established murine acute RIR and OGD/R models to investigate the neuroprotective effects of Ex-4. Our findings revealed that Ex-4 treatment significantly attenuated inner retinal structural damage and loss of RGCs following acute RIR injury. Simultaneously, we demonstrated that GLP-1R antagonist (Ex-9-39) effectively abolished Ex-4-mediated neuroprotection effect, confirming the essential role of GLP-1R activation in this process.

The current study confirmed that the downstream regulatory effects of GLP-1RAs are dependent on the presence of GLP-1R. However, the distribution of GLP-1R in the retinal tissues remains controversial. Zhang et al first demonstrated the presence of GLP-1R in rat retinal tissue using Western blotting (WB) and polymerase chain reaction (PCR).³⁸ Hao et al confirmed GLP-1R expression in RGC-5 cells.³⁹ Hernández et al first characterized GLP-1R expression patterns in human retina, demonstrating its presence in GCL, INL and ONL, with predominant expression observed in GCL.⁴⁰ Contrary to previous reports, Hebsgaard et al demonstrated minimal GLP-1R expression in human retinal tissues (<1% positivity in GCL) using rigorously validated immunohistochemical and in situ hybridization approaches. Meanwhile, Hebsgaard et al also noted that the GLP-1R antibody (ab39072) used by Hernández et al was withdrawn due to its lack of specificity.⁴¹ In a recent study, Wang et al conducted single-cell sequencing of human retinal tissue and found that GLP-1R was not present in human RGCs.⁴² As a G protein-coupled receptor, GLP-1R typically exhibits high degree of homology between different species. In this study, we demonstrated the lack of detectable GLP-1R expression in primary murine RGCs. This finding mechanistically explains our paradoxical observations: while intravitreal Ex-4 administration exerts neuroprotection effect in vivo, Ex-4 treatment shows no significant amelioration of OGD/R-induced RGC damage due to the lack of GLP-1R expression. Taken together with the above studies and the results of this study, we speculate that Ex-4 may exert a protective effect on RGCs under RIR injury through other indirect pathways.

Vascular endothelial cells, which constitute the fundamental structural and functional unit of the vasculature, could promote neuronal survival and angiogenesis by releasing multiple neurotrophic and angiogenic factors, including vascular endothelial growth factor, BDNF, and nerve growth factor.⁴³ Given the inseparable anatomical and functional interplay between the vascular and nervous systems, we postulate that Ex-4 exerts its neuroprotective effects via VECs-mediated pathways. We established a HRVECs/RGCs co-culture system. Our findings demonstrate that HRVECs pretreated with Ex-4 substantially attenuated OGD/R-induced RGCs injury in co-culture systems. These results delineate a novel paracrine protective mechanism whereby Ex-4 protects RGCs under OGD/R condition by modulating VECs function, suggesting a neurovascular unit-mediated pathway of protection.

VECs-derived EVs, a newly recognized form of angiocrine signaling, have been shown to be protective in various human diseases such as cardiovascular diseases.⁴⁴ Given the relatively easy ex vivo culture of ECs, VECs-derived EVs represent promising therapeutic candidates for IR-induced neuronal injury. Our data indicated that primary RGCs could internalize EVs secreted from endothelial cells. However, the dynamic monitoring of this process and precise intracellular localization of EVs in RGCs remain further investigation. Accumulating evidence indicates that miRNAs serve as the central mediator of intercellular signaling via EVs across a broad range of experimental settings.^{45–47} To investigate which exosomal miRNA confers protective effects on RGCs under acute RIR injury, we collected O-EVs and E-EVs for miRNA sequencing analysis. miR-450b-5p has been studied in ischemia/reperfusion injury in heart, kidney, liver and brain tissue.^{32,48–50} At the same time plasma exosome miR-450b-5p has been found to be a potential biomarker and therapeutic target for transient ischemic attack in rats.⁵¹ Our study identified miR-450b-5p as a key mediator of E-EVs-induced protective role of RGCs under acute RIR injury. However, we do not completely exclude the contribution of other differentially expressed miRNAs (miR-191-5p, miR-30d-5p, miR-323a-3p, miR-11980 and miR-3648) and other EV components (eg, proteins, lipids) to this neuroprotective effect, which is worth of further investigation.

Conclusions

In summary, we propose the use of Ex-4, a well-established antidiabetic agent, as a potential therapeutic intervention for neuroinjury following acute RIR. Our findings reveal that Ex-4 exhibits neuroprotective potential beyond its conventional role in diabetes and its complications. From a neurovascular perspective, we investigated the neuroprotective mechanisms of Ex-4 and identified miR-450b-5p in E-EVs as a key regulatory target for RGC damage. This study demonstrates that Ex-4 as a promising therapeutic candidate for IR-induced ocular neurodegeneration, with potential applications extending to broader ischemic neurological conditions.

Acknowledgments

This study was supported by the National Natural Science Foundation of China (82070957, 82101124, and 82201226). The funders were not involved in any aspect of the study, including design, data collection, analysis, interpretation, or manuscript preparation.

Disclosure

The authors report no conflicts of interest in this work.

References

- Zhang M, Liu Q, Meng H, et al. Ischemia-reperfusion injury: molecular mechanisms and therapeutic targets. *Signal Transduct Target Ther.* 2024;9(1):12. doi:10.1038/s41392-023-01688-x
- Antonetti DA, Lin CM, Shanmugam S, et al. Diabetes renders photoreceptors susceptible to retinal ischemia-reperfusion injury. *Invest Ophthalmol Vis Sci.* 2024;65(13):46. doi:10.1167/iovs.65.13.46
- Wan P, Su W, Zhang Y, et al. LncRNA H19 initiates microglial pyroptosis and neuronal death in retinal ischemia/reperfusion injury. *Cell Death Differ.* 2020;27(1):176–191. doi:10.1038/s41418-019-0351-4
- Nakahara T, Hoshino M, Hoshino S, Mori A, Sakamoto K, Ishii K. Structural and functional changes in retinal vasculature induced by retinal ischemia-reperfusion in rats. *Exp Eye Res.* 2015;135:134–145. doi:10.1016/j.exer.2015.02.020
- Wilson CA, Berkowitz BA, Funatsu H, et al. Blood-retinal barrier breakdown following experimental retinal ischemia and reperfusion. *Exp Eye Res.* 1995;61(5):547–557. doi:10.1016/S0014-4835(05)80048-X
- Osborne NN, Casson RJ, Wood JP, Chidlow G, Graham M, Melena J. Retinal ischemia: mechanisms of damage and potential therapeutic strategies. *Prog Retin Eye Res.* 2004;23(1):91–147. doi:10.1016/j.preteyeres.2003.12.001
- Qin Q, Yu N, Gu Y, et al. Inhibiting multiple forms of cell death optimizes ganglion cells survival after retinal ischemia reperfusion injury. *Cell Death Dis.* 2022;13(5):507. doi:10.1038/s41419-022-04911-9
- Nauck MA, Quast DR, Wefers J, Meier JJ. GLP-1 receptor agonists in the treatment of type 2 diabetes state-of-the-art. *Mol Metab.* 2021;46:101102. doi:10.1016/j.molmet.2020.101102
- Tsutsumi YM, Tsutsumi R, Hamaguchi E, et al. Exendin-4 ameliorates cardiac ischemia/reperfusion injury via caveolae and caveolins-3. *Cardiovasc Diabetol.* 2014;13(1):132. doi:10.1186/s12933-014-0132-9
- Chien CT, Jou MJ, Cheng TY, Yang CH, Yu TY, Li PC. Exendin-4-loaded PLGA microspheres relieve cerebral ischemia/reperfusion injury and neurologic deficits through long-lasting bioactivity-mediated phosphorylated Akt/eNOS signaling in rats. *J Cereb Blood Flow Metab.* 2015;35(11):1790–1803. doi:10.1038/jcbfm.2015.126
- Chang YC, Hsu SY, Yang CC, et al. Enhanced protection against renal ischemia-reperfusion injury with combined melatonin and exendin-4 in a rodent model. *Exp Biol Med.* 2016;241(14):1588–1602. doi:10.1177/1535370216642528
- Basalay MV, Mastitskaya S, Mrochek A, et al. Glucagon-like peptide-1 (GLP-1) mediates cardioprotection by remote ischaemic conditioning. *Cardiovasc Res.* 2016;112(3):669–676. doi:10.1093/cvr/cvz216
- Zhai R, Xu H, Hu F, Wu J, Kong X, Sun X. Exendin-4, a GLP-1 receptor agonist regulates retinal capillary tone and restores microvascular patency after ischaemia-reperfusion injury. *Br J Pharmacol.* 2020;177(15):3389–3402. doi:10.1111/bph.15059
- Rocha-Ferreira E, Poupon L, Zelco A, et al. Neuroprotective exendin-4 enhances hypothermia therapy in a model of hypoxic-ischaemic encephalopathy. *Brain.* 2018;141(10):2925–2942. doi:10.1093/brain/awy220
- Femminella GD, Frangou E, Love SB, et al. Evaluating the effects of the novel GLP-1 analogue liraglutide in Alzheimer's disease: study protocol for a randomised controlled trial (ELAD study). *Trials.* 2019;20(1):191. doi:10.1186/s13063-019-3259-x
- Athauda D, Gulyani S, Karnati HK, et al. Utility of neuronal-derived exosomes to examine molecular mechanisms that affect motor function in patients with Parkinson disease: a secondary analysis of the exenatide-PD trial. *JAMA Neurol.* 2019;76(4):420–429. doi:10.1001/jamaneurol.2018.4304
- Kaur C, Foulds WS, Ling EA. Blood-retinal barrier in hypoxic ischaemic conditions: basic concepts, clinical features and management. *Prog Retin Eye Res.* 2008;27(6):622–647. doi:10.1016/j.preteyeres.2008.09.003
- Kim H, Li Q, Hempstead BL, Madri JA. Paracrine and autocrine functions of brain-derived neurotrophic factor (BDNF) and nerve growth factor (NGF) in brain-derived endothelial cells. *J Biol Chem.* 2004;279(32):33538–33546. doi:10.1074/jbc.M404115200
- Zhang YZ, Liu F, Song CG, et al. Exosomes derived from human umbilical vein endothelial cells promote neural stem cell expansion while maintain their stemness in culture. *Biochem Biophys Res Commun.* 2018;495(1):892–898. doi:10.1016/j.bbrc.2017.11.092
- Yokoi A, Villar-Prados A, Oliphant PA, et al. Mechanisms of nuclear content loading to exosomes. *Sci Adv.* 2019;5(11):8849. doi:10.1126/sciadv.aax8849
- Chen CC, Liu L, Ma F, et al. Elucidation of exosome migration across the blood-brain barrier model in vitro. *Cell Mol Bioeng.* 2016;9(4):509–529. doi:10.1007/s12195-016-0458-3
- Venkat P, Cui C, Chopp M, et al. MiR-126 mediates brain endothelial cell exosome treatment-induced neurorestorative effects after stroke in type 2 diabetes mellitus mice. *Stroke.* 2019;50(10):2865–2874. doi:10.1161/STROKEAHA.119.025371
- Yue KY, Zhang PR, Zheng MH, et al. Neurons can upregulate Cav-1 to increase intake of endothelial cells-derived extracellular vesicles that attenuate apoptosis via miR-1290. *Cell Death Dis.* 2019;10(12):869. doi:10.1038/s41419-019-2100-5
- Barres BA, Silverstein BE, Corey DP, Chun LL. Immunological, morphological, and electrophysiological variation among retinal ganglion cells purified by panning. *Neuron.* 1988;1(9):791–803. doi:10.1016/0896-6273(88)90127-4
- Meyer-Franke A, Kaplan MR, Pfrieger FW, Barres BA. Characterization of the signaling interactions that promote the survival and growth of developing retinal ganglion cells in culture. *Neuron.* 1995;15(4):805–819. doi:10.1016/0896-6273(95)90172-8
- Zhang X, Wei M, Fan J, et al. Ischemia-induced upregulation of autophagy precludes dysfunctional lysosomal storage and associated synaptic impairments in neurons. *Autophagy.* 2021;17(6):1519–1542. doi:10.1080/15548627.2020.1840796
- Huang CC, Narayanan R, Alapati S, Ravindran S. Exosomes as biomimetic tools for stem cell differentiation: applications in dental pulp tissue regeneration. *Biomaterials.* 2016;111:103–115. doi:10.1016/j.biomaterials.2016.09.029
- Sohel MM, Hoelker M, Noferesti SS, et al. Exosomal and non-exosomal transport of extra-cellular micromas in follicular fluid: implications for bovine oocyte developmental competence. *PLoS One.* 2013;8(11):e78505. doi:10.1371/journal.pone.0078505
- Meng M, Chaquour B, O'Neill N, et al. Comparison of Brn3a and RBPMs labeling to assess retinal ganglion cell loss during aging and in a model of optic neuropathy. *Invest Ophthalmol Vis Sci.* 2024;65(4):19. doi:10.1167/iovs.65.4.19

30. Catalano M, O'Driscoll L. Inhibiting extracellular vesicles formation and release: a review of EV inhibitors. *J Extracell Vesicles*. 2019;9(1):1703244. doi:10.1080/20013078.2019.1703244
31. Li M, Meng Z, Yu S, et al. Baicalein ameliorates cerebral ischemia-reperfusion injury by inhibiting ferroptosis via regulating GPX4/ACSL4/ACSL3 axis. *Chem Biol Interact*. 2022;366:110137. doi:10.1016/j.cbi.2022.110137
32. Yu Q, Zhang N, Gan X, et al. EGCG attenuated acute myocardial infarction by inhibiting ferroptosis via miR-450b-5p/ACSL4 axis. *Phytomedicine*. 2023;119:154999. doi:10.1016/j.phymed.2023.154999
33. Li Y, Feng D, Wang Z, et al. Ischemia-induced ACSL4 activation contributes to ferroptosis-mediated tissue injury in intestinal ischemia/reperfusion. *Cell Death Differ*. 2019;26(11):2284–2299. doi:10.1038/s41418-019-0299-4
34. Drucker DJ. Mechanisms of action and therapeutic application of glucagon-like peptide-1. *Cell Metab*. 2018;27(4):740–756. doi:10.1016/j.cmet.2018.03.001
35. Teramoto S, Miyamoto N, Yatomi K, et al. Exendin-4, a glucagon-like peptide-1 receptor agonist, provides neuroprotection in mice transient focal cerebral ischemia. *J Cereb Blood Flow Metab*. 2011;31(8):1696–1705. doi:10.1038/jcbfm.2011.51
36. Shan Y, Tan S, Lin Y, et al. The glucagon-like peptide-1 receptor agonist reduces inflammation and blood-brain barrier breakdown in an astrocyte-dependent manner in experimental stroke. *J Neuroinflammation*. 2019;16(1):242. doi:10.1186/s12974-019-1638-6
37. Xie Z, Enkhjargal B, Wu L, et al. Exendin-4 attenuates neuronal death via GLP-1R/PI3K/Akt pathway in early brain injury after subarachnoid hemorrhage in rats. *Neuropharmacology*. 2018;128:142–151. doi:10.1016/j.neuropharm.2017.09.040
38. Zhang Y, Wang Q, Zhang J, Lei X, Xu GT, Ye W. Protection of exendin-4 analogue in early experimental diabetic retinopathy. *Graefes Arch Clin Exp Ophthalmol*. 2009;247(5):699–706. doi:10.1007/s00417-008-1004-3
39. Hao M, Kuang HY, Fu Z, Gao XY, Liu Y, Deng W. Exenatide prevents high-glucose-induced damage of retinal ganglion cells through a mitochondrial mechanism. *Neurochem Int*. 2012;61(1):1–6. doi:10.1016/j.neuint.2012.04.009
40. Hernandez C, Bogdanov P, Corraliza L, et al. Topical administration of GLP-1 receptor agonists prevents retinal neurodegeneration in experimental diabetes. *Diabetes*. 2016;65(1):172–187. doi:10.2337/db15-0443
41. Hebsgaard JB, Pyke C, Yildirim E, Knudsen LB, Heegaard S, Kvist PH. Glucagon-like peptide-1 receptor expression in the human eye. *Diabetes Obes Metab*. 2018;20(9):2304–2308. doi:10.1111/dom.13339
42. Wang SK, Nair S, Li R, et al. Single-cell multiome of the human retina and deep learning nominate causal variants in complex eye diseases. *Cell Genom*. 2022;2(8):100164. doi:10.1016/j.xgen.2022.100164
43. Garcia-Bonilla L, Moore JM, Racchumi G, et al. Inducible nitric oxide synthase in neutrophils and endothelium contributes to ischemic brain injury in mice. *J Immunol*. 2014;193(5):2531–2537. doi:10.4049/jimmunol.1400918
44. Nakahashi T, Fujimura H, Altar CA, et al. Vascular endothelial cells synthesize and secrete brain-derived neurotrophic factor. *FEBS Lett*. 2000;470(2):113–117. doi:10.1016/S0014-5793(00)01302-8
45. Xin H, Katakowski M, Wang F, et al. MicroRNA cluster miR-17-92 cluster in exosomes enhance neuroplasticity and functional recovery after stroke in rats. *Stroke*. 2017;48(3):747–753. doi:10.1161/STROKEAHA.116.015204
46. Teng Y, Ren Y, Hu X, et al. MVP-mediated exosomal sorting of miR-193a promotes colon cancer progression. *Nat Commun*. 2017;8(1):14448. doi:10.1038/ncomms14448
47. Sakha S, Muramatsu T, Ueda K, Inazawa J. Exosomal microRNA miR-1246 induces cell motility and invasion through the regulation of DENND2D in oral squamous cell carcinoma. *Sci Rep*. 2016;6(1):38750. doi:10.1038/srep38750
48. Huang Z, Mou T, Luo Y, et al. Inhibition of miR-450b-5p ameliorates hepatic ischemia/reperfusion injury via targeting CRYAB. *Cell Death Dis*. 2020;11(6):455. doi:10.1038/s41419-020-2648-0
49. Kim JM, Byun JS, Kim J, et al. Analysis of microRNA signatures in ischemic stroke thrombus. *J Neurointerv Surg*. 2022;14(5):017597. doi:10.1136/neurintsurg-2021-017597
50. Luo X, Wang W, Li D, et al. Plasma Exosomal miR-450b-5p as a possible biomarker and therapeutic target for transient ischaemic attacks in rats. *J Mol Neurosci*. 2019;69(4):516–526. doi:10.1007/s12031-019-01341-9
51. Xin H, Li Y, Cui Y, Yang JJ, Zhang ZG, Chopp M. Systemic administration of exosomes released from mesenchymal stromal cells promote functional recovery and neurovascular plasticity after stroke in rats. *J Cereb Blood Flow Metab*. 2013;33(11):1711–1715. doi:10.1038/jcbfm.2013.152

International Journal of Nanomedicine

Publish your work in this journal

The International Journal of Nanomedicine is an international, peer-reviewed journal focusing on the application of nanotechnology in diagnostics, therapeutics, and drug delivery systems throughout the biomedical field. This journal is indexed on PubMed Central, MedLine, CAS, SciSearch®, Current Contents®/Clinical Medicine, Journal Citation Reports/Science Edition, EMBASE, Scopus and the Elsevier Bibliographic databases. The manuscript management system is completely online and includes a very quick and fair peer-review system, which is all easy to use. Visit <http://www.dovepress.com/testimonials.php> to read real quotes from published authors.

Submit your manuscript here: <https://www.dovepress.com/international-journal-of-nanomedicine-journal>

Dovepress
Taylor & Francis Group